HHS Public Access

Author manuscript

Acc Chem Res. Author manuscript; available in PMC 2016 February 17.

Published in final edited form as:

Acc Chem Res. 2015 February 17; 48(2): 286–294. doi:10.1021/ar500362y.

Positron Emission Tomography Imaging Using Radiolabeled Inorganic Nanomaterials

Xiaolian Sun[†,‡,*], **Weibo Cai**[§,*], and **Xiaoyuan Chen**[‡,*]

[†]Center for Molecular Imaging and Translational Medicine, State Key Laboratory of Molecular Vaccinology and Molecular Diagnostics, School of Public Health, Xiamen University, Xiang'an South Road, Xiamen 361102, China

[‡]Laboratory of Molecular Imaging and Nanomedicine, National Institute of Biomedical Imaging and Bioengineering, National Institutes of Health, Bethesda, Maryland 20892, United States

[§]Departments of Radiology and Medical Physics, University of Wisconsin—Madison, Madison, Wisconsin 53706, United States

CONSPECTUS

Positron emission tomography (PET) is a radionuclide imaging technology that plays an important role in preclinical and clinical research. With administration of a small amount of radiotracer, PET imaging can provide a noninvasive, highly sensitive, and quantitative readout of its organ/tissue targeting efficiency and pharmacokinetics. Various radiotracers have been designed to target specific molecular events. Compared with antibodies, proteins, peptides, and other biologically relevant molecules, nanoparticles represent a new frontier in molecular imaging probe design, enabling the attachment of different imaging modalities, targeting ligands, and therapeutic payloads in a single vector.

[*]Corresponding Authors: Xiaolian Sun, xiaolian.sun@nih.gov., Weibo Cai, WCai@uwhealth.org., Xiaoyuan Chen, shawn.chen@nih.gov.

Author Contributions

The manuscript was written through contributions of all authors. All authors have given approval to the final version of the manuscript. All authors contributed equally.

Notes

The authors declare no competing financial interest.

We introduce the radiolabeled nanoparticle platforms that we and others have developed. Due to the fundamental differences in the various nanoparticles and radioisotopes, most radiolabeling methods are designed case-by-case. We focus on some general rules about selecting appropriate isotopes for given types of nanoparticles, as well as adjusting the labeling strategies according to specific applications. We classified these radiolabeling methods into four categories: (1) complexation reaction of radiometal ions with chelators via coordination chemistry; (2) direct bombardment of nanoparticles via hadronic projectiles; (3) synthesis of nanoparticles using a mixture of radioactive and nonradioactive precursors; (4) chelator-free postsynthetic radiolabeling. Method 1 is generally applicable to different nanomaterials as long as the surface chemistry is well-designed. However, the addition of chelators brings concerns of possible changes to the physicochemical properties of nanomaterials and detachment of the radiometal. Methods 2 and 3 have improved radiochemical stability. The applications are, however, limited by the possible damage to the nanocomponent caused by the proton beams (method 2) and harsh synthetic conditions (method 3). Method 4 is still in its infancy. Although being fast and specific, only a few combinations of isotopes and nanoparticles have been explored. Since the applications of radiolabeled nanoparticles are based on the premise that the radioisotopes are stably attached to the nanomaterials, stability (colloidal and radiochemical) assessment of radiolabeled nanoparticles is also highlighted.

Despite the fact that thousands of nanomaterials have been developed for clinical research, only very few have moved to humans. One major reason is the lack of understanding of the biological behavior of nanomaterials. We discuss specific examples of using PET imaging to monitor the *in vivo* fate of radiolabeled nanoparticles, emphasizing the importance of labeling strategies and caution in interpreting PET data. Design considerations for radiolabeled nanoplatforms for multimodal molecular imaging are also illustrated, with a focus on strategies to combine the strengths of different imaging modalities and to prolong the circulation time.

1. INTRODUCTION

Molecular imaging, which is defined as "*in vivo* visualization, characterization and measurement of biological process at the molecular and cellular level", has played an important role in diagnosing and monitoring diseases.[1] Positron emission tomography (PET) is a highly sensitive and noninvasive nuclear imaging technology widely used for preclinical and clinical imaging of diseases.[2] Upon the injection of imaging probes labeled with radionuclides that emit positrons, PET imaging can monitor their distribution and concentration: the positron emitted from nucleus eventually collides with a nearby negatively charged electron. During the annihilation, two 511 keV γ-rays in the direction about 180° apart are produced and detected by a PET scanner. The images of γ-rays obtained by the PET scanner can reflect the distribution and concentration of isotopes.[2]

PET imaging of radiolabeled nanoparticles has generated great excitement in the field of molecular imaging. Nano-particles refer to materials with at least one dimension ranging from a few to several hundred nanometers. Many recent reviews have provided a good overview of the advantages of nanoparticles as molecular imaging agents, including but not limited to their unique physical properties and ease of surface functionalization.[3–5] In this Account, we mainly focus on nanoparticles with an inorganic core. From the perspective of PET imaging agents, compared with biologically relevant molecules, nanoparticles have a large surface area-to-volume ratio and are capable of loading or attaching a variety of targeting, diagnostic, or therapeutic agents in a single vector. Targeting agents could provide enhanced receptor binding specificity and affinity and thus more accurately detect indicative molecular markers of various diseases. Different diagnostic agents could help overcome the limitations of single-modality imaging and synergistically improve the diagnostic accuracy/quality. In addition, the longer half-life of nano-particles over free drug molecules also leads to an enhanced bioavailability.[6,7] Despite the ever expanding development of nanoparticle-based imaging agents, most applications are limited to animal models. Concerns about how the body will actually metabolize nanomaterials and whether prolonged exposure to nanomaterials will induce long-term toxicity have greatly slowed their progress toward clinical trials.[6–9] The complexity of nanoparticles makes it very challenging to understand the biological path and fate in living subjects. With its high sensitivity and the ability to conduct quantitative analysis of noninvasive whole-body images, PET, in turn, is an excellent choice to explore the *in vivo* fate of nanoparticles.

This Account will introduce our efforts over the past decade in the design and construction of radiolabeled nanoparticles and describe their wide applications from disease diagnosis to evaluating their biological fate.

2. CONSTRUCTION OF RADIOLABELED NANOPARTICLES

The successful construction of a radiolabeled nanoparticle platform includes three segments: an appropriate isotope, a well-functionalized nanoparticle, and an efficient and reliable labeling method to connect these two.

2.1. Choice of Isotope

Table 1 summarizes some representative radioisotopes for nanoparticle labeling. To choose the suitable radioisotopes, four aspects need to be taken into consideration: (1) imaging characteristics of isotopes; (2) decay half-life; (3) isotope availability; (4) reliability of radiolabeling strategy. Low positron energy and high branching ratio of β^+ decay are favorable decay characteristics for PET imaging. Isotopes with high positron energy will have a large travel distance before positron annihilating and thus have a loss of spatial resolution. Isotopes with low positron efficiency, that is, a low fraction of atoms undergo β^+ decay among the decay of overall atoms, require long scan times and often obtain noisy images.[10] The decay half-life of radioisotopes is also of great concern. Compared with short half-life radionuclides such as ^{13}N ($t_{1/2}$ = 9.97 min), ^{68}Ga ($t_{1/2}$ = 67.7 min), and ^{18}F ($t_{1/2}$ = 109.8 min), radionuclides with longer half-lives such as ^{64}Cu ($t_{1/2}$ = 12.7 h), ^{72}As ($t_{1/2}$ = 26 h), and ^{89}Zr ($t_{1/2}$ = 78.4 h) are more flexible for complex radiolabeling processes and more suitable for transportation to institutes lacking radiochemistry facilities. For cancer imaging purposes, the half-life of the isotopes should match the biological half-life of the vectors to allow them to reach the target of interest. It is also important that the decay time is as short as possible in order to avoid unnecessary radiation exposure. However, in order to study the fate of administered nanomaterials with prolonged circulation, relatively long-lived isotopes are preferred for monitoring the clearance profile. When it comes to isotope availability, besides the possibilities for the center to obtain the isotopes (either from its own radiochemistry facility or transport from other PET centers), noting that the production yield could vary from several μCi/μAh to several mCi/μAh depending on different isotopes and nuclear reactions. Last but not least, the isotope should be stably attached or loaded to the vectors.

2.2. Radiolabeling Method

An ideal radiolabeling method should be robust, quick, safe, and highly efficient and should produce minimal change to the original properties of the nanoparticles. The principle of “as low as reasonably achievable (ALARA)” guides the entire radioactive material handling process.[23] High reaction temperature, prolonged reaction time, and a complicated purification method, which pose a threat for both the properties of nanoparticles and the health of operators, should be avoided. With a good number of radiolabeling methods available, it is not possible to claim which method is best. The selection of labeling methods should therefore be based on the specific radioisotope, research purpose, and practicability.

Here, we divide these radiolabeling methods into four categories (Figure 1): (1) complexation reaction of radiometal ions with chelators via coordination chemistry; (2) direct bombardment of nanoparticles via hadronic projectiles; (3) synthesis of nanoparticles using a mixture of radioactive and nonradioactive precursors; (4) chelator-free postsynthetic radiolabeling.

Coordination of the radiometal via a chelator (Figure 1a) is the most widely used radiolabeling strategy until now. A wide range of radiometal ions with different nuclear properties are available for various applications. Traditionally, the radiometal–chelator complex is directly attached to vectors such as peptides and antibodies.[24] There are two

important considerations when conjugating radiometal to nanoparticles: surface functionalization of nanoparticles[4] and chelation of radiometal.[25] A strong binding between radiolabeled surfactants (or other biocompatible molecules used) and the nanoparticle surface is desirable to avoid the detachment of surfactants from the nanoparticle. It is also required that the radiometal forms a stable coordination complex with the chelator to minimize the transchelation of radiometal (section 2.3). This approach is generally applicable to different nanomaterials with the help of well-designed surface chemistry and is relatively easy to operate. The primary concerns include the possible detachment of radiometals caused via either dissociation of surfactant or transchelation of radiometal, as well as the change of physicochemical properties after chelator modification.

The unique properties of inorganic nanoparticles allow radiolabeling without the help of chelators. For instance, bombarding nanoparticles with hadronic projectiles such as protons and neutrons can directly radiolabel nanoparticles (Figure 1b).[26] In a typical example, direct proton irradiation has been applied to ^{18}O enriched Al_2O_3 nanoparticles to produce Al_2O_3 containing ^{13}N via the $^{18}O(p,\alpha)^{13}N$ nuclear reaction without affecting the crystal structure or other properties of the nanoparticles.[11] Since the radioisotope is incorporated inside the nanoparticles, the signal is believed to truly reflect the distribution of nanoparticles without leaking. However, this synthetic concept is greatly limited by the access to the proton beams. In addition, the exposure to protons and concurrent neutrons during such process might affect the properties of the nanoparticles, especially when the surface of nanoparticles is conjugated with biologically active molecules. Thus, the application prospects of this method are limited.

An alternative method to incorporate radioisotopes inside nanoparticles is to use radioactive precursors to synthesize intrinsically radioactive nanoparticles (Figure 1c). Since the radioactive precursors are typically at the trace level (in the range of picomolar to nanomolar concentration), they are usually mixed with normal nonradioactive precursors. It is generally believed that the radioisotopes are built-inside the crystal lattice of the normal nanocrystals, resulting in high radiochemical stability. $^{198}Au^{3+}$, a SPECT (single-photon emission computed tomography) isotope, is a typical radioisotope that is suitable for this labeling strategy.[27,28] It has a high reduction potential and thus can be easily reduced under mild conditions. The relatively long half-life (3.14 days) provides adequate time for the transportation of ^{198}Au from the reactor facility as well as preparation and purification of the synthesized radioactive nanoparticles.

^{64}Cu ($t_{1/2}$ = 12.7 h) is the most widely used PET radionuclide for this strategy. [^{64}Cu]CuS nanoparticles have been prepared by metathesis reaction of $^{64}CuCl_2$, $CuCl_2$, and Na_2S at 95 °C for 1 h.[16] Coheating of $^{64}CuCl_2$, gold chloride, and copper acetylacetonate in oleylamine at 160 °C for 2 h produced 10 nm [^{64}Cu]Au nanoparticles.[18] Another example is the production of [^{64}Cu]Fe_3O_4 by microvave-assisted heating via hydrolysis of $^{64}CuCl_2$, $FeCl_2$, and $FeCl_3$.[17] Compared with ^{198}Au, the chemical reactivity of ^{64}Cu is relatively low. Thus, nanoparticle synthesis involving ^{64}Cu usually requires higher temperature and longer incubation time, which, to some extent, increases the risk of radiation contamination. Other isotopes used for direct synthesis of nanoparticles (such as ^{111}In[29] and ^{109}Cd[30]) also share the same concerns of harsh synthetic conditions.

Although in this Account, we focus on inorganic nano-particles for PET imaging applications, it is worth mentioning that radiometals together with some organic molecules can also be used as precursors to produce intrinsically radiolabeled organic nanoparticles. Usually these organic molecules have high affinity for metal ions and can self-assemble into nanoplatforms. For example, by simple mixing of $^{64}Cu^{2+}$ with a mixture of heavy and light ferritin chains in an acidic environment and adjustment of the pH back to 7.4, $^{64}Cu^{2+}$ trapped ferritin nanocages are formed.[31] The strong binding site for divalent cations in the center of the pores prevents $^{64}Cu^{2+}$ from escaping, and the ferritin cage can prevent alien "invasion" such as serum to access the $^{64}Cu^{2+}$.

Chelator-free postsynthetic radiolabeling is an emerging concept for radiolabeling nanoparticles (Figure 1d). It takes advantage of the specific physical or chemical interaction between certain radioisotopes and nanoparticles to integrate isotopes into as-prepared nanoparticles with minimal influence on their original properties. It is especially significant when the coordination chemistry is not available for the radionuclides. For instance, nonmetal radioisotopes $*As^{III}$ and $*As^{V}$ (* = 71, 72, 74, or 76) are difficult to incorporate into imaging vectors via coordination chemistry. However, they can be trapped by magnetite with high efficiency via the formation of stable As complexes. Thus, the Cai group designed a chelator-free labeling method by simply mixing *As and iron oxide nanoparticles (IONPs).[21] The labeling of *As was proven to be highly specific to IONPs (blocking the IONP surface with a layer of dense silica or using nonmetal oxide NPs (e.g., CuS) resulted in negligible *As labeling) with a relatively fast and iron-concentration-dependent labeling reaction pattern (84.2% labeling yield within 2 h; specific radioactivity ca. 3.0 MBq μmol^{-1} of Fe). The same strategy has also been successfully applied to ^{69}Ge,[32] another isotope that is unsuitable for radiolabeling via standard coordination chemistry. After coating the radiolabeled IONPs with poly(ethylene glycol) (PEG), around 55% *As and 75% ^{69}Ge were intact after 24 h incubation with whole mouse serum at 37 °C. Although the stability still needs to be improved in future optimization studies, the easy-to-accomplish, fast-and-efficient labeling method has great significance in biomedical applications (e.g., sentinel lymph node mapping with PET and MRI).

In the hope of finding a general approach to label different nanoparticles, we also explored chemical methods for postsynthetic radiolabeling. Cation exchange reactions have been utilized for decades to transform ionic nanocrystals into other components with limited change to their original morphology.[33] For example, Cu can be encapsulated into ionic quantum dots (QDs) via a place exchange between Cu^{+} and the original cation. Using this reaction, we have successfully doped a trace amount of ^{64}Cu radioisotope into CdSe/ZnS core/shell QDs with a labeling yield reaching 100% within 1 h.[19] We found that Cu could replace Zn and even diffuse inside the core to replace Cd under mild reaction conditions. The interaction between ^{64}Cu and QDs was proven to be strong with negligible release of ^{64}Cu after incubation in fetal bovine serum at 37 °C for 48 h. This approach is applicable to a series of QDs with different sizes and emission wavelengths. Recently, we successfully used N_2H_4, a mild reducing agent, to deposit the reduced ^{64}Cu onto the surface of PEG-stabilized Au nanoparticles at room temperature regardless of their shapes and sizes.[20] The distribution of Au nanoparticles in rodents quantified by the Au amount in tissue

homogenate via elemental analysis is linearly correlated with the distribution of ^{64}Cu radioactivity, confirming the reliability of [^{64}Cu]Au nanoparticles for *in vivo* PET imaging. The mild synthetic conditions not only exerted no change on the physical properties of Au nanoparticles but also maintained the bioactivity of the conjugated ligands during the entire labeling process.

The chelator-free postsynthetic radiolabeling strategy is fast and specific and usually can achieve high labeling yield under mild reaction conditions. However, until now this strategy has only been successfully applied to limited combinations of isotopes and nanoparticles.

2.3. Stability of Radiolabeled Nanoparticles

Stability has two meanings for radiolabeled nanoparticles: the colloidal stability and the radiochemical stability. Excellent colloidal stability is a prerequisite of all nanoparticle-based imaging agents. Nanoparticle platforms are usually surface-engineered with polymers for water solubility, tags for imaging, and ligands for target recognition. The hydrodynamic size comprises all of the above as well as the adsorbed proteins and ions in the biological system. A reasonable hydrodynamic size with an acceptable deviation during their lifetime is a feature of colloidally stable nanoparticles.[34]

Radiochemical stability is also critical for radiolabeled nanoparticles. Since PET imaging detects the localization of the radionuclide, in order to truly reflect the distribution of vectors, the radionuclides have to be stably linked to the vectors. Thermodynamic stability of the radioisotope–vector complex is essential in evaluating the labeling efficiency under specific conditions.[35] Kinetic dissociation in the presence of biological competitive ions, serum proteins, and enzymes is also required to predict the *in vivo* stability.[35] Considering the complexity of nanoparticles including size, shape, surface charge, and multiple attachments, there is no unified and well-established approach to test radiochemical stability of nanoparticles. Usually, radiolabeled nanoparticles are incubated in different media (PBS or mouse serum with or without ethylenediaminetetraacetic acid (EDTA)) at 37 °C over time, and the detached radionuclide is evaluated via size exclusion HPLC, iTLC, disposable PD-10 size exclusion columns, or centrifugal filtration.[36] The choice of medium can be tricky. The use of PBS with different pH values can test chemical binding without considering the notorious radiometal dissociation culprits such as biologically relevant chelators like serum proteins and enzymes. On the other hand, using pure serum or even serum with EDTA as medium, which are well above normal physiological levels, although trustworthy, may be too harsh for the development of new PET probes. The complexity of biological systems makes it unlikely to counterfeit a medium with proper amounts of biological chelators. Therefore, strictly speaking, it is not accurate to use a single *in vitro* measurement to predict the *in vivo* radiochemical stability of probes. Instead, *in vivo* experiments are more authentic. Some detached radiometal or radiometal labeled polymer would be rapidly excreted from mice via the renal route over several hours,[37] resulting in strong radioactivity signal in the bladder. Some unstable labeling has a persistent uptake of detached radio-nuclides in certain organs (e.g., ^{89}Zr in the bone[38]), which can be easily distinguished from nanoparticles. For radionuclides that share the same target organ with nanoparticles (e.g., ^{64}Cu in the liver[39]), a second means is highly desirable to analyze the

distribution of nanoparticles; the radiochemical stability can be judged by the discrepancy of the distribution of nanoparticles and radionuclides (section 3).

3. MONITORING THE BIOLOGICAL FATE OF NANOPARTICLES VIA PET

For biomedical use of nanomaterials, it is necessary to understand the "absorption, distribution, metabolism, and excretion" (ADME) pattern of materials in order to strike a balance between the nanoparticle-induced benefits and the possible long-term toxicity caused by exposure to nano-particles.[40–42] PET imaging has unique advantages of high sensitivity and the ability to conduct quantitative analysis of whole-body imaging; hence it is undoubtedly a convenient tool to quantify the biodistribution of nanoparticles. Instead of sacrificing mice at different time points and measuring each tissue, PET imaging monitors the nanoparticles in a continuous and noninvasive manner. Considering the diverse properties of nanoparticles, labeling nanoparticles by coordinating the radiometal with a chelator is still the preferred option. There is often a concern of the possible detachment of radiometals, requiring an alternative method to distinguish between the signal originating from nanoparticles versus that from the radionuclide.

We have exploited the combination of macrocyclic chelating agent 1,4,7,10-tetraazacyclododecane-1,4,7,10-tetraacetic acid (DOTA) and radionuclide ^{64}Cu to label various nanoparticles. ^{64}Cu is selected due to its relatively long decay half-life (12.7 h), which is comparable to the circulation time of many types of nanoparticles (mostly several hours), decay properties (β^+, 0.653 MeV, 17.8%; β^-, 0.579 MeV, 38.4%; the remainder is electron capture), and the well-established coordination chemistry.[15] DOTA is widely used because of the commercial availability of many different bifunctional DOTA derivatives that can be easily conjugated to a variety of surfactants for different nanoparticles and because of its acceptable stability.[43] For instance, we functionalized single-walled carbon nanotubes (SWCNTs) noncovalently with phospholipid-PEG-NH_2 and labeled them with DOTA for ^{64}Cu chelation and PET imaging[44] (Figure 2a). No detachment of ^{64}Cu was observed after incubation in full mouse serum over 24 h, and no rapid excretion of ^{64}Cu[45] or ^{64}Cu-labeled polymer[37] was observed from mice via the renal route in the first few hours. Furthermore, the amount of SWCNTs in each tissue derived from their intrinsic Raman signals is a good match with the PET data based on radioactivity of ^{64}Cu (Figure 2c), confirming that PET imaging is able to reflect the biodistribution of SWCNTs. With the help of PET, the biodistribution and circulation of SWCNTs with different surface modifications are clearly seen (Figure 2b): lower liver and spleen uptakes and longer blood circulation time were observed for SWCNTs coated with PEG of 5.4 kDa ($t_{1/2} \approx 2$ h) than those with PEG of 2 kDa ($t_{1/2} \approx 0.5$ h). After further conjugation with arginine-glycine-aspartic acid (RGD) peptide, a targeting ligand for cancer biomarker integrin $\alpha_v\beta_3$, SWCNT-PEG_{5400}-RGD showed a tumor uptake as high as 10–15% of the injected dose (ID)/g, compared with only 3–4%ID/g for SWCNT-PEG_{5400} (without the targeting ligand, RGD).

In another study, to explain the effect of CNTs on fetal development after injection to pregnant mice, we used PET to observe the biodistribution and translocation of CNTs.[46] We used the same procedure mentioned above to label SWCNTs and multiwalled carbon nanotubes (MWCNTs) with similar lengths but different outer diameters (<8, 20–30, and 50

nm). After intravenous injection into pregnant mice, we found obvious accumulation of all four samples in the uterus of pregnant mice (Figure 2d). *Ex vivo* imaging of the isolated fetuses also confirmed the accumulation of CNTs in the fetal liver and placenta with negligible difference among these samples (Figure 2e,f). These results helped us conclude that CNTs could penetrate mouse placental tissues and directly affect fetal development and growth.

4. RADIOLABELED NANOPARTICLES FOR MOLECULAR IMAGING

As emerging imaging agents, nanoparticles have two major advantages. On the one hand, different imaging modalities can be integrated into a single nanoparticle platform. Each imaging modality has its own advantages and disadvantages. For example, although PET imaging is very sensitive (down to picomolar level) and quantitative, its resolution (typical >1 mm) is relatively low. Magnetic resonance imaging (MRI) has a submillimeter-level spatial resolution but inherently low sensitivity. Optical imaging is highly sensitive and easily accessible. However, the scatter of light limits its penetration depth and spatial resolution. Thus, combining the strengths of different imaging modalities can synergistically improve the imaging quality. On the other hand, nanomaterials with appropriate functionalization can evade attack from the immune system and thus have prolonged circulation time. Multiple targeting ligands can further be conjugated to a single nanoparticle and provide enhanced receptor binding affinity via a polyvalency effect.[47] In this Account, we only focus on the imaging agents with radionuclides for tumor imaging applications.

We take QDs as an example to illustrate the design considerations for the imaging probes. QDs are intrinsically attractive fluorescent probes for biological imaging due to their unique optical properties such as size- and composition-dependent fluorescence emission wavelength, high quantum yield, and high photostability. However, the information from *in vivo* fluorescence signals is only qualitative or at best semiquantitative. Thus, we labeled the amine functionalized QD surface with DOTA for ^{64}Cu chelation and quantitative PET imaging.[48] Results from *in vivo* PET, *ex vivo* PET, *ex vivo* near-infrared fluorescence (NIRF) imaging, and tissue homogenate fluorescence closely correlated. This indicates the reliability of using *in vivo* PET to quantify the distribution of this dual functional QD-based probe. To improve the tumor uptake, we further conjugated cancer-targeting ligands such as RGD[48] and VEGF[49] to the amine functionalized QDs. Cell-binding assays and cell staining experiments proved that RGD and VEGF maintained their integrin $\alpha_v\beta_3$- and VEGF receptor (VEGFR)-specific binding after conjugation. *In vivo* PET showed a significantly higher U87MG (overexpressing both integrin $\alpha_v\beta_3$ and VEGFR) tumor uptake of ^{64}Cu-DOTA-QDs-RGD and ^{64}Cu-DOTA-QDs-VEGF than of ^{64}Cu-DOTA-QDs.

Besides the capability for dual modality PET/NIRF imaging, radiolabeled QDs also allow Cerenkov resonance energy transfer (CRET).[50] Positron emitting radionuclides like ^{64}Cu can produce Cerenkov luminescence (CL).[51] CL serves as an internal light source that will not be affected by the light-absorption/scattering properties of biological tissue and autofluorescence background. QDs can help convert the CL, which is intense in blue/ultraviolet wavelengths to a longer wavelength, which is more suitable for *in vivo* imaging. The CRET efficiency is dependent on the ratio of energy donor (radioisotope) to energy

acceptor (QDs), as well as the distance between these two. We designed a CRET system by doping ^{64}Cu inside QDs via cation exchange reaction[19] (section 2.2, Figure 3). The 100% labeling yield makes it possible to optimize the ^{64}Cu-to-QD ratio simply by tuning the input amount of ^{64}Cu for radiolabeling. Our results showed that with the same amount of ^{64}Cu radioactivity and QDs, doping ^{64}Cu inside QDs greatly improved the CRET efficiency. This results in a 2-fold higher light intensity around the QD emission wavelength than that of the mixture of ^{64}Cu and QDs, while free ^{64}Cu has no obvious peak at the expected 636 nm wavelength. One major advantage of this approach is that ^{64}Cu was doped inside QDs, which eliminated potential dissociation of the radionuclide-chelated polymer from the nanoparticles. The amount of QDs in the tissue homogenate obtained by elemental analysis was consistent with the ^{64}Cu radioactivity level in the same tissue. In addition, the nonchelated surface of ^{64}Cu-doped QDs was favorable for further conjugation. Although there is no direct evidence that co-conjugating different agents on the same surface would affect their functionalities, possible cross-linking is indeed a concern for coupling agents with commonly used functional groups (e.g., RGD-NH_2 and DOTA-COOH). Besides QDs, we also explored Au nanoclusters, which have high fluorescence and excellent biocompatibility as CRET acceptors.[52] The ^{64}Cu integrated Au nanoclusters have a tumor uptake as high as 15.2%ID/g at 24 h postinjection and have been successfully used for *in vivo* synergistic dual-modality PET and CRET-NIR imaging.

Other radiolabeled nanoparticles that have been investigated for tumor imaging include but are not limited to IONPs, mesoporous silica NPs (MSNs), Au nanoparticles, and graphene oxide nanoparticles. Each has its unique imaging or therapeutic capability. Specific examples can be found in several recent reviews.[53,54] From our point of view, radiochemical stability is highly important for the construction of PET imaging agents. This becomes especially significant when imaging vectors are further conjugated with therapeutic agents for imaging-guided therapy. The information on the exact amount of therapeutic agents inside the tumor is critical for the development of personalized therapeutic protocols to reduce the side effects. Furthermore, more attention should also be paid to increasing the tumor targeting ability and imaging quality of nanoparticles.

It has been proposed that prolonging the circulation time can provide more opportunity for nanoparticles to access the cancer cells. Therefore, we used human serum albumin (HSA), a robust and native protein in the body, to extend the circulation half-life of IONPs.[55] We have encapsulated IONPs in HSA matrices and further conjugated the amine groups of HSA with Cy5.5 fluorescent dye and DOTA for ^{64}Cu chelation to make them MRI/PET/NIRF triple active (Figure 4a,b). Quantitative analysis of PET imaging demonstrated that at the same dose (10 mg Fe/kg), mice injected with HSA-coated IONPs had a gradually enhanced liver uptake over the 24 h period, in stark contrast to the maximum liver uptake at 1 h for mice injected with IONPs without HSA. This result indicates that HSA coating successfully protects IONPs from macrophage uptake and subsequent hepatic clearance and improves their circulation half-life.

In another study, we have prepared a 60 nm MRI/NIRF/PET trimodel imaging nanoplatform based on MSNs.[56] The NIRF dye was doped into the MSNs via dye-labeled MSN precursors. Subsequently, Gd^{3+} ions, a commonly used T_1 MRI contrast agent, were loaded

into the pore channels of MSNs by mixing the MSNs with $GdCl_3$ solution and protected by hyaluronic acid-based polymer (HA). PET imaging agent $^{64}Cu^{2+}$ was then integrated into the nanoplatform by DOTA chelation. Bone-marrow derived mesenchymal stem cells (MSCs) were successfully labeled with these MSNs (Figure 4c) for multimodal imaging of the homing of MSCs to tumors in an orthotopic U87MG glioblastoma model (Figure 4d).

5. CONCLUSIONS

PET imaging using radiolabeled nanoparticles plays an important role in translating nanotechnology research into future biomedical/clinical practice. The capabilities of nano-particles to load different functionalities endow them with many advantages over bioactive molecule based radiotracers. There are two major benefits of the quantitative nature of PET. First, it provides an understanding of the biological fate of nanoparticles predicting the ADME pattern of materials of the same sort (composition, size, shape, surface chemistry, etc.). Second, it optimizes the physicochemical properties of nanoparticles to fit the specific biomedical applications. The diverse structures of nanoparticles have led to a variety of radiolabeling methods. However, the development of properly radiolabeled nanoparticles is still at an early stage necessitating a reliable and unified guideline in the near future. When different labeling methods are used to label specific nano-particles for a given application or purpose, it is always essential to incorporate radioisotopes onto nanoparticles with minimal impact on their original biological behavior. Multidisciplinary and concerted effort from a variety of entities (e.g., funding agencies, regulatory authorities, clinicians, scientists, etc.) will be needed to quickly move nanotechnology into clinical translation for the benefit of patients.

Acknowledgments

Funding

We thank the intramural research program of the National Institute of Biomedical Imaging and Bioengineering (NIBIB), the University of Wisconsin—Madison, the National Institutes of Health (Grant NIBIB/NCI 1R01CA169365), the Department of Defense (Grant W81XWH-11-1-0644), and the American Cancer Society (Grant 125246-RSG-13-099-01-CCE) for the support of this work.

We thank Dr. Iqbal Ali for her proof-reading of the manuscript.

References

1. Mankoff DA. A definition of molecular imaging. J Nucl Med. 2007; 48:18N–21N.
2. Gambhir SS. Molecular imaging of cancer with positron emission tomography. Nat Rev Cancer. 2002; 2:683–693. [PubMed: 12209157]
3. Ma X, Zhao Y, Liang XJ. Theranostic nanoparticles engineered for clinic and pharmaceutics. Acc Chem Res. 2011; 44:1114–1122. [PubMed: 21732606]
4. Xie J, Liu G, Eden HS, Ai H, Chen X. Surface-engineered magnetic nanoparticle platforms for cancer imaging and therapy. Acc Chem Res. 2011; 44:883–892. [PubMed: 21548618]
5. Cheon J, Lee JH. Synergistically integrated nanoparticles as multimodal probes for nanobiotechnology. Acc Chem Res. 2008; 41:1630–1640. [PubMed: 18698851]
6. Choyke PL. Nanoparticles: Take only pictures, leave only footprints. Sci Transl Med. 2014; 6(260fs44)
7. Chow EK-H, Ho D. Cancer nanomedicine: From drug delivery to imaging. Sci Transl Med. 2013; 5(216rv4)

8. Phillips E, Penate-Medina O, Zanzonico PB, Carvajal RD, Mohan P, Ye Y, Humm J, Gönen M, Kalaigian H, Schöder H, Strauss HW, Larson SM, Wiesner U, Bradbury MS. Clinical translation of an ultrasmall inorganic optical-PET imaging nanoparticle probe. Sci Transl Med. 2014; 6(260ra149)
9. Lavik E, von Recum H. The role of nanomaterials in translational medicine. ACS Nano. 2011; 5:3419–3424. [PubMed: 21604811]
10. Ametamey SM, Honer M, Schubiger PA. Molecular imaging with PET. Chem Rev. 2008; 108:1501–1516. [PubMed: 18426240]
11. Pérez-Campaña C, Gómez-Vallejo V, Puigivila M, Martín A, Calvo-Fernández T, Moya SE, Ziolo RF, Reese T, Llop J. Biodistribution of different sized nanoparticles assessed by positron emission tomography: A general strategy for direct activation of metal oxide particles. ACS Nano. 2013; 7:3498–3505. [PubMed: 23473535]
12. Burke BP, Clemente GS, Archibald SJ. Recent advances in chelator design and labelling methodology for 68Ga radiopharmaceuticals. J Labelled Compd Radiopharm. 2014; 57:239–243.
13. Perez-Campana C, Gomez-Vallejo V, Martin A, San Sebastian E, Moya SE, Reese T, Ziolo RF, Llop J. Tracing nanoparticles in vivo: A new general synthesis of positron emitting metal oxide nanoparticles by proton beam activation. Analyst. 2012; 137:4902–4906. [PubMed: 22957337]
14. Liu Q, Sun Y, Li C, Zhou J, Li C, Yang T, Zhang X, Yi T, Wu D, Li F. 18F-labeled magnetic-upconversion nanophosphors via rare-earth cation-assisted ligand assembly. ACS Nano. 2011; 5:3146–3157. [PubMed: 21384900]
15. Shokeen M, Anderson CJ. Molecular imaging of cancer with copper-64 radiopharmaceuticals and positron emission tomography (PET). Acc Chem Res. 2009; 42:832–841. [PubMed: 19530674]
16. Zhou M, Zhang R, Huang M, Lu W, Song S, Melancon MP, Tian M, Liang D, Li C. A chelator-free multifunctional [64Cu] CuS nanoparticle platform for simultaneous micro-PET/CT imaging and photothermal ablation therapy. J Am Chem Soc. 2010; 132:15351–15358. [PubMed: 20942456]
17. Wong RM, Gilbert DA, Liu K, Louie AY. Rapid size-controlled synthesis of dextran-coated, 64Cu-doped iron oxide nanoparticles. ACS Nano. 2012; 6:3461–3467. [PubMed: 22417124]
18. Zhao Y, Sultan D, Detering L, Cho S, Sun G, Pierce R, Wooley KL, Liu Y. Copper-64-alloyed gold nanoparticles for cancer imaging: Improved radiolabel stability and diagnostic accuracy. Angew Chem, Int Ed. 2014; 53:156–159.
19. Sun X, Huang X, Guo J, Zhu W, Ding Y, Niu G, Wang A, Kiesewetter DO, Wang ZL, Sun S. Self-illuminating 64Cu-doped CdSe/ZnS nanocrystals for in vivo tumor imaging. J Am Chem Soc. 2014; 136:1706–1709. [PubMed: 24401138]
20. Sun X, Huang X, Yan X, Wang Y, Guo J, Jacobson O, Liu D, Szajek LP, Zhu W, Niu G. Chelator-free 64Cu-integrated gold nanomaterials for positron emission tomography imaging guided photothermal cancer therapy. ACS Nano. 2014; 8:8438–8446. [PubMed: 25019252]
21. Chen F, Ellison PA, Lewis CM, Hong H, Zhang Y, Shi S, Hernandez R, Meyerand ME, Barnhart TE, Cai W. Chelator-free synthesis of a dual-modality PET/MRI agent. Angew Chem, Int Ed. 2013; 52:13319–13323.
22. Severin WG, Engle WJ, Barnhart ET, Nickles RJ. 89Zr radiochemistry for positron emission tomography. Med Chem. 2011; 7:389–394. [PubMed: 21711221]
23. Prasad KN, Cole WC, Haase GM. Radiation protection in humans: Extending the concept of as low as reasonably achievable (ALARA) from dose to biological damage. Br J Radiol. 2004; 77:97–99. [PubMed: 15010379]
24. Goldenberg DM. Targeted therapy of cancer with radiolabeled antibodies. J Nucl Med. 2002; 43:693–713. [PubMed: 11994535]
25. Wadas TJ, Wong EH, Weisman GR, Anderson CJ. Coordinating radiometals of copper, gallium, indium, yttrium, and zirconium for PET and SPECT imaging of disease. Chem Rev. 2010; 110:2858–2902. [PubMed: 20415480]
26. Gibson N, Holzwarth U, Abbas K, Simonelli F, Kozempel J, Cydzik I, Cotogno G, Bulgheroni A, Gilliland D, Ponti J. Radiolabelling of engineered nanoparticles for in vitro and in vivo tracing applications using cyclotron accelerators. Arch Toxicol. 2011; 85:751–773. [PubMed: 21479952]
27. Black KCL, Wang Y, Luehmann HP, Cai X, Xing W, Pang B, Zhao Y, Cutler CS, Wang LV, Liu Y, Xia Y. Radioactive 198Au-doped nanostructures with different shapes for in vivo analyses of

their biodistribution, tumor uptake, and intratumoral distribution. ACS Nano. 2014; 8:4385–4394. [PubMed: 24766522]

28. Wang Y, Liu Y, Luehmann H, Xia X, Wan D, Cutler C, Xia Y. Radioluminescent gold nanocages with controlled radioactivity for real-time in vivo imaging. Nano Lett. 2013; 13:581–585. [PubMed: 23360442]
29. Zeng J, Jia B, Qiao R, Wang C, Jing L, Wang F, Gao M. In situ 111In-doping for achieving biocompatible and non-leachable 111In-labeled Fe3O4 nanoparticles. Chem Commun. 2014; 50:2170–2172.
30. Cai W, Hong H. In a "nutshell": Intrinsically radio-labeled quantum dots. Am J Nucl Med Mol Imaging. 2012; 2:136. [PubMed: 23133808]
31. Lin X, Xie J, Niu G, Zhang F, Gao H, Yang M, Quan Q, Aronova MA, Zhang G, Lee S. Chimeric ferritin nanocages for multiple function loading and multimodal imaging. Nano Lett. 2011; 11:814–819. [PubMed: 21210706]
32. Chakravarty R, Valdovinos HF, Chen F, Lewis CM, Ellison PA, Luo H, Meyerand ME, Nickles RJ, Cai W. Intrinsically germanium-69-labeled iron oxide nanoparticles: Synthesis and in-vivo dual-modality PET/MR imaging. Adv Mater. 2014; 26:5119–5123. [PubMed: 24944166]
33. Son DH, Hughes SM, Yin Y, Alivisatos AP. Cation exchange reactions in ionic nanocrystals. Science. 2004; 306:1009–1012. [PubMed: 15528440]
34. Rivera-Gil P, Jimenez De Aberasturi D, Wulf V, Pelaz B, Del Pino P, Zhao Y, De La Fuente JM, Ruiz De Larramendi I, Rojo T, Liang XJ. The challenge to relate the physicochemical properties of colloidal nanoparticles to their cytotoxicity. Acc Chem Res. 2012; 46:743–749. [PubMed: 22786674]
35. Cutler CS, Hennkens HM, Sisay N, Huclier-Markai S, Jurisson SS. Radiometals for combined imaging and therapy. Chem Rev. 2013; 113:858–883. [PubMed: 23198879]
36. Price EW, Orvig C. Matching chelators to radiometals for radiopharmaceuticals. Chem Soc Rev. 2014; 43:260–290. [PubMed: 24173525]
37. Chen X, Hou Y, Tohme M, Park R, Khankaldyyan V, Gonzales-Gomez I, Bading JR, Laug WE, Conti PS. Pegylated Arg-Gly-Asp peptide: 64Cu labeling and PET imaging of brain tumor $\alpha v\beta 3$-integrin expression. J Nucl Med. 2004; 45:1776–1783. [PubMed: 15471848]
38. Zhang Y, Hong H, Cai W. PET tracers based on zirconium-89. Curr Radiopharm. 2011; 4:131. [PubMed: 22191652]
39. Bass LA, Wang M, Welch MJ, Anderson CJ. In vivo transchelation of copper-64 from TETA-octreotide to superoxide dismutase in rat liver. Bioconjugate Chem. 2000; 11:527–532.
40. Soo Choi H, Liu W, Misra P, Tanaka E, Zimmer JP, Itty Ipe B, Bawendi MG, Frangioni JV. Renal clearance of quantum dots. Nat Biotechnol. 2007; 25:1165–1170. [PubMed: 17891134]
41. Choi HS, Ashitate Y, Lee JH, Kim SH, Matsui A, Insin N, Bawendi MG, Semmler-Behnke M, Frangioni JV, Tsuda A. Rapid translocation of nanoparticles from the lung airspaces to the body. Nat Biotechnol. 2010; 28:1300–1303. [PubMed: 21057497]
42. Wang B, He X, Zhang Z, Zhao Y, Feng W. Metabolism of nanomaterials in vivo: Blood circulation and organ clearance. Acc Chem Res. 2012; 46:761–769. [PubMed: 23964655]
43. De León-Rodríguez LM, Kovacs Z. The synthesis and chelation chemistry of DOTA–peptide conjugates. Bioconjugate Chem. 2007; 19:391–402.
44. Liu Z, Cai W, He L, Nakayama N, Chen K, Sun X, Chen X, Dai H. In vivo biodistribution and highly efficient tumour targeting of carbon nanotubes in mice. Nat Nanotechnol. 2006; 2:47–52. [PubMed: 18654207]
45. Peng F, Lu X, Janisse J, Muzik O, Shields AF. PET of human prostate cancer xenografts in mice with increased uptake of 64CuCl2. J Nucl Med. 2006; 47:1649–1652. [PubMed: 17015901]
46. Huang X, Zhang F, Sun X, Choi KY, Niu G, Zhang G, Guo J, Lee S, Chen X. The genotype-dependent influence of functionalized multiwalled carbon nanotubes on fetal development. Biomaterials. 2014; 35:856–865. [PubMed: 24344357]
47. Jokerst JV, Gambhir SS. Molecular imaging with theranostic nanoparticles. Acc Chem Res. 2011; 44:1050–1060. [PubMed: 21919457]

48. Cai W, Chen K, Li ZB, Gambhir SS, Chen X. Dual-function probe for PET and near-infrared fluorescence imaging of tumor vasculature. J Nucl Med. 2007; 48:1862–1870. [PubMed: 17942800]
49. Chen K, Li ZB, Wang H, Cai W, Chen X. Dual-modality optical and positron emission tomography imaging of vascular endothelial growth factor receptor on tumor vasculature using quantum dots. Eur J Nucl Med Mol Imaging. 2008; 35:2235–2244. [PubMed: 18566815]
50. Liu H, Zhang X, Xing B, Han P, Gambhir SS, Cheng Z. Radiation-luminescence-excited quantum dots for in vivo multiplexed optical imaging. Small. 2010; 6:1087–1091. [PubMed: 20473988]
51. Ruggiero A, Holland JP, Lewis JS, Grimm J. Cerenkov luminescence imaging of medical isotopes. J Nucl Med. 2010; 51:1123–1130. [PubMed: 20554722]
52. Hu H, Huang P, Weiss OJ, Yan X, Yue X, Zhang MG, Tang Y, Nie L, Ma Y, Niu G, Wu K, Chen X. PET and NIR optical imaging using self-illuminating 64Cu-doped chelator-free gold nanoclusters. Biomaterials. 2014; 35:9868–9876. [PubMed: 25224367]
53. Xing Y, Zhao J, Conti PS, Chen K. Radiolabeled nanoparticles for multimodality tumor imaging. Theranostics. 2014; 4:290–306. [PubMed: 24505237]
54. Hong H, Zhang Y, Sun J, Cai W. Molecular imaging and therapy of cancer with radiolabeled nanoparticles. Nano Today. 2009; 4:399–413. [PubMed: 20161038]
55. Xie J, Chen K, Huang J, Lee S, Wang J, Gao J, Li X, Chen X. PET/NIRF/MRI triple functional iron oxide nanoparticles. Biomaterials. 2010; 31:3016–3022. [PubMed: 20092887]
56. Huang X, Zhang F, Wang H, Niu G, Choi KY, Swierczewska M, Zhang G, Gao H, Wang Z, Zhu L. Mesenchymal stem cell-based cell engineering with multifunctional mesoporous silica nanoparticles for tumor delivery. Biomaterials. 2013; 34:1772–1780. [PubMed: 23228423]

Biographies

Xiaolian Sun earned her Ph.D. in Chemistry from Brown University in 2012 and then joined the National Institute of Biomedical Imaging and Bioengineering (NIBIB), National Institutes of Health (NIH), as a postdoctoral fellow. Her current research is focused on the design and synthesis of nanomaterial-based imaging probes. She recently secured a faculty position at Xiamen University, China.

Weibo Cai is currently an Associate Professor of Radiology and Medical Physics at the University of Wisconsin—Madison. He received his Ph.D. in Chemistry from UC San Diego in 2004. After postdoctoral training at Stanford University, he launched his career at UW—Madison in early 2008. His research is primarily focused on molecular imaging and nanotechnology (http://mi.wisc.edu/), investigating the biomedical applications of various agents developed in his laboratory for imaging and therapy of cancer and cardiovascular diseases.

Xiaoyuan Chen is a Senior Investigator and Chief of the Laboratory of Molecular Imaging and Nanomedicine (LOMIN), National Institute of Biomedical Imaging and Bioengineering (NIBIB), National Institutes of Health (NIH). His lab aims to develop a molecular imaging toolbox for better understanding of biology, early diagnosis of disease, monitoring therapy response, and guiding drug discovery and development. LOMIN puts special emphasis on high-sensitivity nanosensors for biomarker detection and theranostic nanomedicine for imaging, gene and drug delivery, and monitoring of treatment.

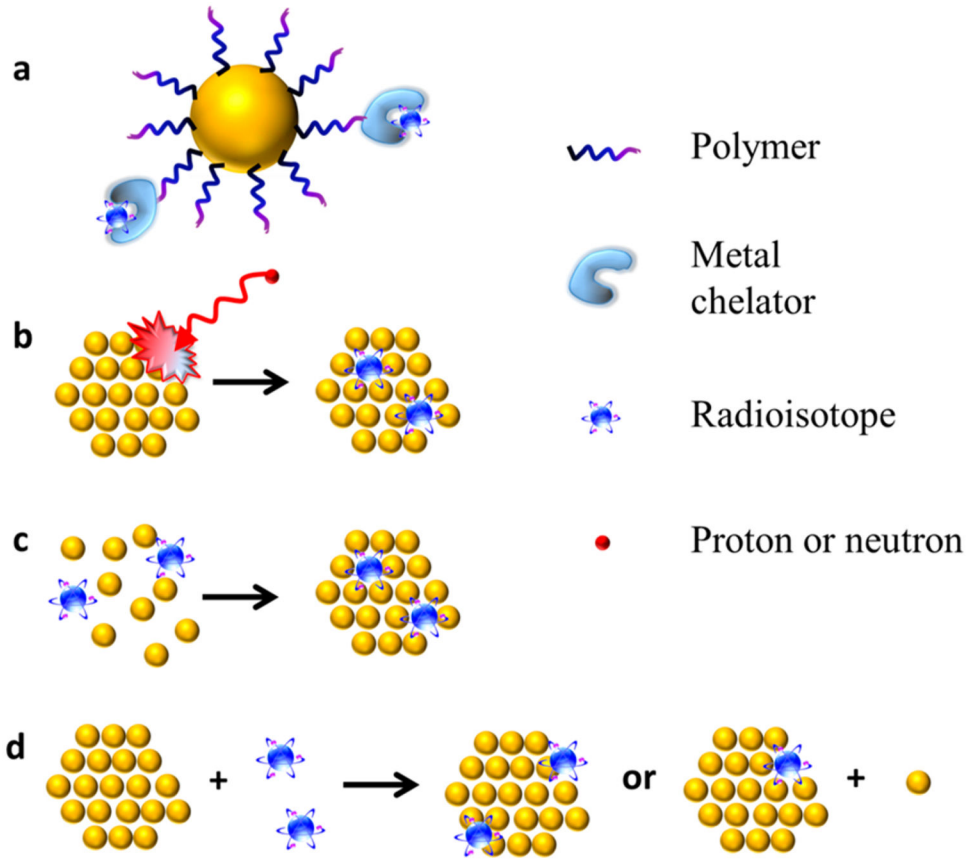

Figure 1.

Schematic drawing of radiolabeled nanoparticles via (a) coordination of radiometal ions with chelators, (b) direct bombardment of nanoparticles with hadronic projectiles, (c) direct synthesis of nanoparticles with radioactive and nonradioactive precursors, and (d) postsynthetic radiolabeling without chelator.

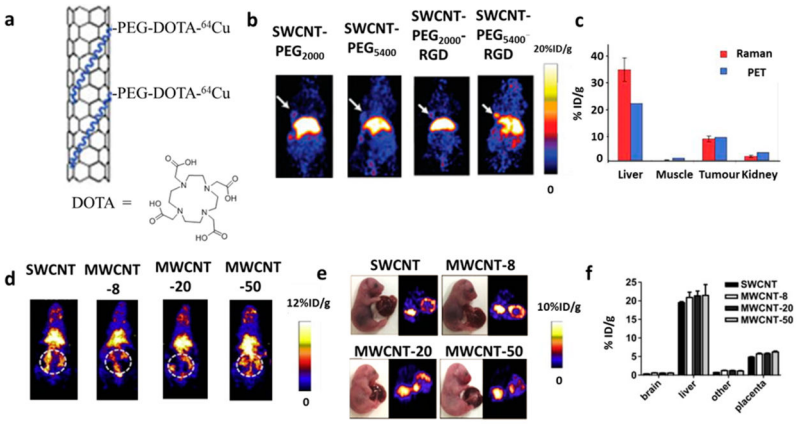

Figure 2.

(a) Scheme of phospholipid-PEG-NH_2 functionalized SWCNTs further labeled with DOTA for ^{64}Cu chelation. (b) Representative PET images of mice at 6 h postinjection of ^{64}Cu-labeled SWCNT-PEG_{2000}, SWCNT-PEG_{5400}, SWCNT-PEG_{2000}-RGD, and SWCNT-PEG_{5400}-RGD, respectively. White arrows indicate the U87MG tumor. Significant differences in the biodistribution and tumor targeting ability were found among the four samples. (c) Biodistribution data at 8 h postinjection of SWCNTs quantified by PET imaging and *ex vivo* Raman spectrometry. Reproduced with permission from ref 44. Copyright 2006 Macmillan Publishers Limited. (d) Representative PET imaging of pregnant mice at 0.5 h postinjection of CNTs. Dashed white circle indicates the uterus. (e,f) *Ex vivo* PET imaging (e) and quantification of the biodistribution (f) of CNTs in fetuses at 48 h postinjection of CNTs. Negligible difference in the fetal liver and placenta uptakes could be found. Reproduced with permission from ref 46. Copyright 2014 Elsevier Ltd.

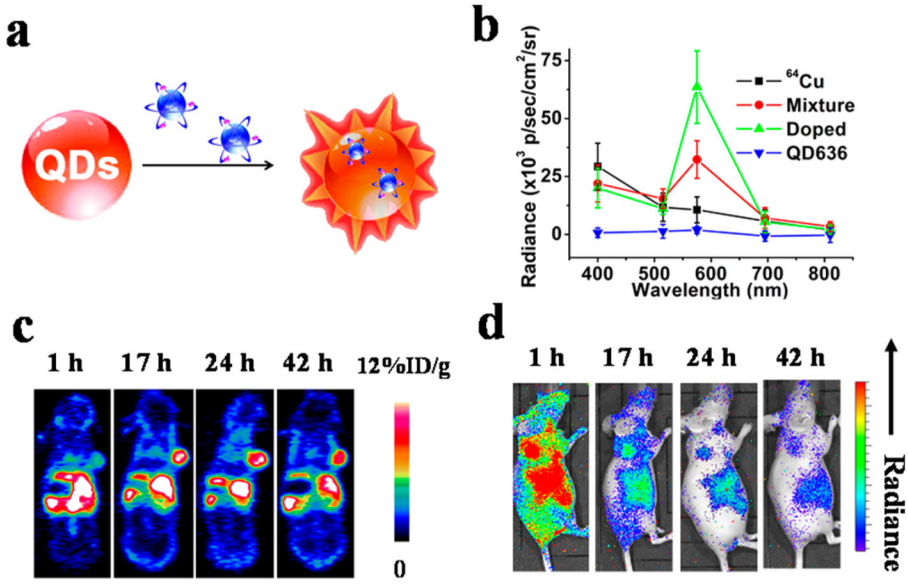

Figure 3.

(a) Design of self-illuminating ^{64}Cu-doped QDs. (b) A typical comparison of photon flux obtained from ^{64}Cu, mixture of ^{64}Cu and QDs, ^{64}Cu-doped QDs, and QDs under different emission filters. ^{64}Cu-doped QDs have an increased photon flux at the emission wavelength of the QDs (636 nm) than the mixture of ^{64}Cu and QDs, indicating a higher Cerenkov resonance energy transfer efficiency. (c, d) Representative whole-body coronal PET (c) and sagittal luminescence imaging (d) of U87MG tumor-bearing mice at 1, 17, 24, and 42 h postinjection of ^{64}Cu-doped QDs. White arrow, tumor area; black arrow, liver area. Reproduced with permission from ref 19. Copyright 2014 American Chemical Society.

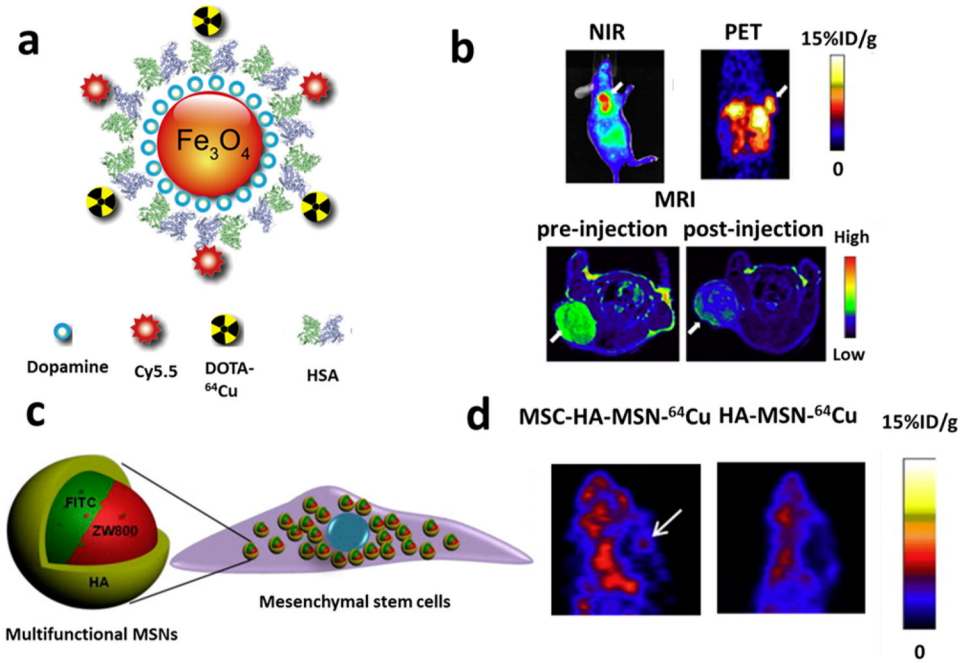

Figure 4.

(a) Schematic illustration of the multifunctional HSA-IONPs. (b) Representative *in vivo* NIR/PET/MRI images of tumor-bearing mice at 18 h postinjection. White arrow, tumor area. Reproduced with permission from ref 55. Copyright 2010 Elsevier Ltd. (c) Schematic illustration of a mesenchymal stem cell (MSC) labeled with MRI/NIRF/PET trimodality mesoporous silica nano-particles (MSNs). (d) PET imaging of orthotopic U87MG glioblastoma homing ability of HA-MSN-^{64}Cu and MSCs labeled with HA-MSN-^{64}Cu 24 h postinjection. The MSC platforms displayed a higher tumor uptake than particles without MSCs. Reproduced with permission from ref 56. Copyright 2013 Elsevier Ltd.

Table 1

Representative Isotopes Suitable for PET Imaging and Their Physical Properties

isotope	half-life	radiation	energy (keV)	NP labeling strategy
^{13}N	9.97 min	β^+ (100%)	1200	Al_2O_3,[11] direct bombardment of nanoparticles
^{68}Ga	67.7 min	β^+ (89%)	770, 1890	coordination via a chelator[12]
^{18}F	109.8 min	β^+ (97%)	634	Al_2O_3,[13] direct bombardment of nanoparticles $NaYF_4$:Gd, Yb, Er[14] chelator-free postsynthetic labeling
^{64}Cu	12.7 h	β^+ (18%)	579, 656	coordination via a chelator[15] CuS,[16] Fe_3O_4,[17] Au[18] radioactive precursor CdSe/ZnS,[19] Au[20] chelator-free postsynthetic labeling
^{72}As	26 h	β^+ (77%)	3430	Fe_3O_4[21] chelator-free postsynthetic labeling
^{89}Zr	78.4 h	β^+ (23%)	908	coordination via a chelator[22]